EurJIC European Journal of Inorganic Chemistry

FULL PAPER

DOI: 10.1002/ejic.201101166

Physical Properties of Eu^{2+}-Containing Cryptates as Contrast Agents for Ultrahigh-Field Magnetic Resonance Imaging

Joel Garcia,[a] Akhila N. W. Kuda-Wedagedara,[a] and Matthew J. Allen*[a]

Keywords: Imaging agents / Magnetic resonance imaging / Cryptands / Lanthanides

The kinetic stabilities and relaxivities of a series of Eu^{2+}-containing cryptates have been investigated. Transmetallation studies, which monitored the change in the longitudinal relaxation rate of water protons in the presence of Ca^{2+}, Mg^{2+}, and Zn^{2+}, demonstrated that the cryptate structure influenced the stability, and two of the cryptates studied were inert to transmetallation in the presence of these endogenous ions. The efficacy of these cryptates was determined at different magnetic field strengths, temperatures, and pH values. Cryptate relaxivity was found to be higher at ultrahigh field strengths (7 and 9.4 T) relative to clinically relevant field strengths (1.4 and 3 T), but the efficiency of these cryptates decreased as the temperature increased. In addition, a variation in pH did not yield significant changes in the efficacy of the cryptates. These studies establish a foundation of important properties that are necessary to develop effective positive contrast agents for magnetic resonance imaging from Eu^{2+}-containing cryptates.

Introduction

Most paramagnetic contrast agents for magnetic resonance imaging (MRI) are used to improve the inherent contrast in MR images by increasing the relaxation rates of the water protons. This ability of Gd^{3+}-based contrast agents to alter the relaxation rates, known as relaxivity, decreases at ultrahigh field strengths.[1] Although Eu^{2+}-containing complexes have been explored as contrast agents in the past,[2] we have recently shown that Eu^{2+}-containing cryptates outperform Gd^{3+} 1,4,7,10-tetraazacyclododecane-*N*,*N*′,*N*″,*N*‴-tetraacetate (GdDOTA) at ultrahigh field strengths.[3] Here, we describe measurements of the kinetic stability of Eu^{2+}-containing cryptates and the influence of magnetic field strengths, temperature, and pH values on their relaxivity.

Kinetic stability, which relates to the inertness of a complex to transmetallation in vivo, is a critical parameter for contrast agents. Weaver and coworkers have reported the stability of cryptate Eu-**1** in the presence of Na^+, Ba^{2+}, and tetraethylammonium cations, which are components of electrolytes in cyclic voltammetric experiments.[4] However, the kinetic stability of Eu^{2+}-containing cryptates in the presence of biologically relevant ions, which include Ca^{2+}, Mg^{2+}, and Zn^{2+}, is of the utmost importance due to the toxicity of uncomplexed europium.[5] Therefore, our kinetic studies explored the stability of the Eu^{2+}-containing complexes of cryptands **1**–**4**, which contain a variety of functional groups (Scheme 1), in the presence of Ca^{2+}, Mg^{2+}, and Zn^{2+}. The use of these ligands allowed us to establish the relationship between the ligand structure and kinetic stability. Additionally, understanding the structural characteristics of Eu^{2+}-containing cryptates that influence relaxivity as a function of pH value, temperature, and magnetic field strength is important because this knowledge should enable the design of improved ligands for use at ultrahigh field strengths.

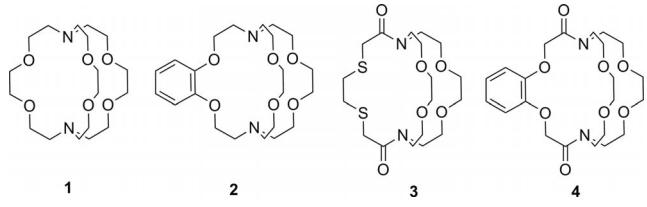

Scheme 1. Structures of **1**–**4**.

Results and Discussion

Synthesis

To synthesize cryptands **3** and **4**, a two-step synthetic procedure was used that involved thionyl chloride and 1,4,10,13-tetraoxa-7,16-diazacyclooctadecane (diazacrown ether). Briefly, the diacids were converted into diacid chlorides followed by immediate reaction with diazacrown ether to produce the desired cryptands (Scheme 2).

[a] Department of Chemistry, Wayne State University,
5101 Cass Avenue, Detroit, MI 48202, USA
Fax: +1-313-577-8822
E-mail: mallen@chem.wayne.edu

Supporting information for this article is available on the WWW under http://dx.doi.org/10.1002/ejic.201101166.

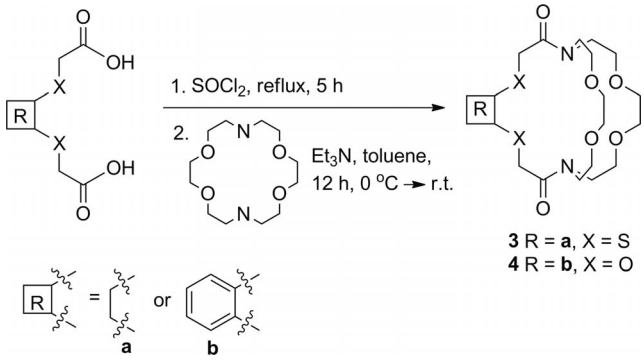

Scheme 2. Synthesis of **3** and **4**.

Kinetic Stability Studies

One critical feature of a useful contrast agent is its stability towards dechelation under physiological conditions. Although the thermodynamic stability constant of Eu-**1** is high ($\log K = 13.0$),[6] kinetic stability is also crucial to evaluate the possibility of demetallation of contrast agents in the presence of endogenous ions. For a small-molecule contrast agent to be used in vivo, it should be kinetically inert for at least long enough to be excreted ($t_{1/2} \approx 5$–6 min in mice, $t_{1/2} \approx 90$ min in humans).[7] Kinetic stability is important because uncomplexed Eu^{2+} oxidizes to Eu^{3+} more easily than Eu^{2+} that is encapsulated in cryptands,[8] and Eu^{3+} is toxic.[5] Prior to excretion, one possible pathway for the release of Eu^{2+} is through transmetallation with endogenous ions. Ions that are found in blood plasma include Ca^{2+}, Mg^{2+}, and Zn^{2+} and these are of particular concern because of their abundance in serum and their tendency to be complexed by ligands. Uncomplexed Ca^{2+} and Mg^{2+} ions, despite having a lower affinity than Zn^{2+} for many ligands,[9] are present in higher concentrations than Zn^{2+} in blood serum (1.05, 1.34, and 0.125 mM for Ca^{2+}, Mg^{2+}, and Zn^{2+}, respectively).[9,10] However, the relatively low concentration of zinc in serum is sufficient to displace gadolinium in diethylenetriamine pentaacetate.[9,11] Therefore, we have examined the stability of Eu^{2+}-containing cryptates **1**–**4** towards transmetallation by monitoring the change in the longitudinal relaxation rate of water protons at 60 MHz in the presence of Ca^{2+}, Mg^{2+}, and Zn^{2+} following the procedure of Muller and coworkers.[9,11] An Eu^{2+}-containing complex was prepared in degassed phosphate buffered saline (PBS) and other metals were added to the solution. The Eu^{2+} complexes are soluble in PBS, however, uncomplexed Eu^{2+} is insoluble, and upon transmetallation, it immediately precipitates.[12] Once Eu^{2+} precipitates, a measurable decrease in the relaxation rate of the water protons is detected. A plot of the ratio of the longitudinal relaxation rates (R_1^p) of the Eu^{2+}-containing solutions at a time (t) relative to initial values ($t = 0$) vs. t allows the extent of transmetallation to be monitored. Muller and coworkers have developed this technique as a way to measure the degree of transmetallation in terms of the kinetic index, which is defined as the time required to reach 80% of the initial longitudinal relaxation rate of water protons. We used concentrations of Ca^{2+}, Mg^{2+}, and Zn^{2+} that are 2.38, 1.87, and 20 times greater than normal in vivo levels, respectively, and the results of our experiments are shown in Figures 1, 2, and 3.

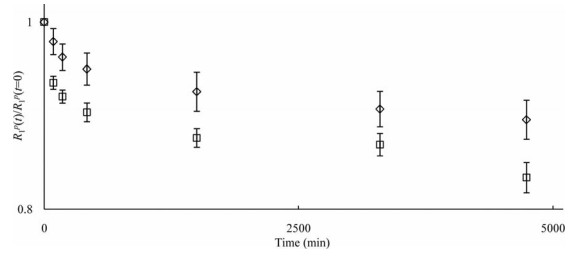

Figure 1. Evolution of $R_1^p(t)/R_1^p(t = 0)$ vs. t for Eu-**1** (◇) and Eu-**2** (□) (2.5 mM) in the presence of Ca^{2+} (2.5 mM). The value 0.8 on the y axis is the threshold for the kinetic index. Error bars represent standard error of the mean.

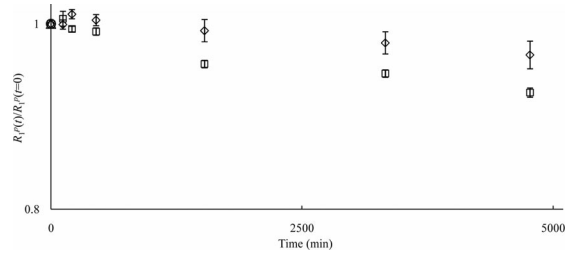

Figure 2. Evolution of $R_1^p(t)/R_1^p(t = 0)$ vs. t for Eu-**1** (◇) and Eu-**2** (□) (2.5 mM) in the presence of Mg^{2+} (2.5 mM). The value 0.8 on the y axis is the threshold for the kinetic index. Error bars represent standard error of the mean.

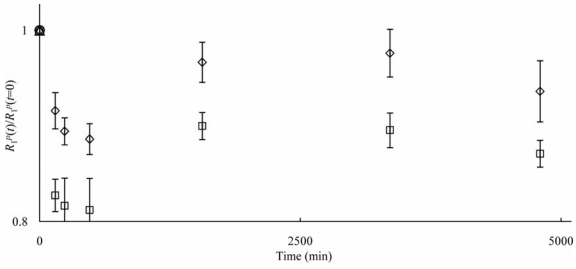

Figure 3. Evolution of $R_1^p(t)/R_1^p(t = 0)$ vs. t for Eu-**1** (◇) and Eu-**2** (□) (2.5 mM) in the presence of Zn^{2+} (2.5 mM). The value 0.8 on the y axis is the threshold for the kinetic index. Error bars represent standard error of the mean.

As seen from the ratio of the longitudinal relaxation rates vs. t (Figures 1, 2, and 3), the kinetic indices of Eu-**1** and Eu-**2** are greater than 4740 min in the presence of Ca^{2+}, Mg^{2+}, and Zn^{2+}(Table 1), which is more than 53 times longer than the half-life of small molecules in vivo. This kinetic index indicates that Eu-**1** and Eu-**2** did not fall below 80% of their efficacy during this time, which suggests that these complexes are inert to transmetallation in the presence of Ca^{2+}, Mg^{2+}, and Zn^{2+} at greater than normal in vivo levels. Interestingly, the values in the presence of Zn^{2+} appeared to decrease initially and then increase again; however, analysis of the variance revealed that all of the data points for Eu-**1** and Eu-**2** in the presence of Zn^{2+} are

not different (α = 0.01). The stability of these Eu^{2+}-containing complexes is likely due to the effective binding of the cryptand to the metal ion.

Table 1. Kinetic indices [min] for Eu-**1**–**4**.

Complex	Ca^{2+}	Mg^{2+}	Zn^{2+}
Eu-**1**	> 4740	> 4770	> 4800
Eu-**2**	> 4740	> 4770	> 4800
Eu-**3**	< 90	< 120	< 240
Eu-**4**	< 90	< 120	< 240

Although Eu-**1** and Eu-**2** showed stability towards transmetallation in the presence of endogenous metal ions, precipitates were observed as soon as PBS was added to Eu-**3** and Eu-**4**, consequently, these data are not included in Figures 1, 2, and 3. This observation suggests a weaker interaction between Eu^{2+} and amide-containing **3** and **4** relative to **1** and **2**. A further decrease in the longitudinal relaxation rate was observed in the presence of Ca^{2+}, Mg^{2+}, and Zn^{2+}. Studies with **3** and **4** were stopped once the longitudinal relaxation rate fell below 80% of the initial value.

The weak binding of Eu^{2+} to **3** and **4** can be attributed to the presence of amide groups in the cryptand structure. Amides have resonance structures (Figure 4) that change both the electronic and structural properties of the ligands relative to **1** and **2**. Because of the presence of partial positive charges on nitrogen atoms, it is unlikely that these nitrogen atoms serve as donors. Thus, the denticity of **3** and **4** is decreased relative to that of **1** and **2**. Furthermore, when the lone pairs on the nitrogen atoms are delocalized, the geometry of the nitrogen atoms changes from pyramidal to trigonal planar, and this change in geometry could also make it harder for Eu^{2+} to coordinate with **3** and **4** relative to **1** and **2**. Consequently, a decrease in the kinetic stability is observed. Because of the ineffective complexation of Eu^{2+} by amide-containing **3** and **4**, we did not include Eu-**3** and Eu-**4** in the relaxometric studies described below. Although amide-containing cryptands are not good ligands for Eu^{2+}, Eu-**1** and Eu-**2** were observed to have high kinetic stabilities in the presence of Ca^{2+}, Mg^{2+}, and Zn^{2+} in concentrations higher than those found in vivo, a promising result for their potential use as contrast agents.

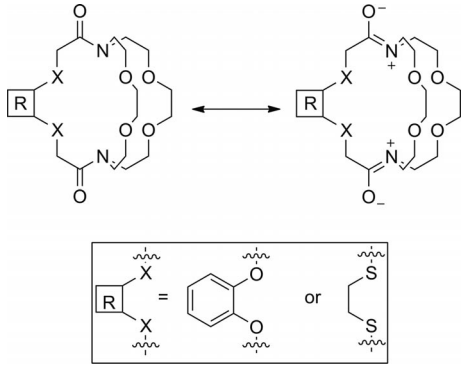

Figure 4. Contributing resonance structures of **3** and **4**.

Proton Relaxometry

Influence of Magnetic Field Strength on Relaxivity

Eu^{2+}-containing cryptates have desirable features that include the presence of two inner-sphere water molecules and fast water-exchange rates, which are two key factors that influence relaxivity. These cryptates are two of a few examples of paramagnetic materials that demonstrate an increase in relaxivity at ultrahigh field strengths relative to lower field strengths.[3,13] To establish a more complete understanding of the behavior of the efficacy of these cryptates as a function of field strength, we measured the relaxivity of Eu-**1** and Eu-**2** at field strengths of 1.4, 3, 7, 9.4, and 11.7 T. These measurements allowed us to compare the efficiency of Eu^{2+}-containing complexes at clinically relevant field strengths (1.4 and 3 T) with that at higher field strengths, which are commonly used in preclinical research (> 3 T). Because relaxivity is dependent on temperature,[14] we compared field strengths at the same temperature.

On comparing the efficacy of Eu^{2+}-containing cryptates at field strengths of 3, 7, 9.4, and 11.7 T (20 °C, pH = 7.4), the relaxivity of Eu-**2** is higher than that of Eu-**1** at all field strengths (Figure 5). This difference in relaxivity is likely due to the difference in rotational correlation rate, which is the rate at which these molecules tumble in solution. This rate is proportional to the molecular weight for structurally similar compounds.[15] The relaxivity of Eu-**1** increases from 3 to 7 T followed by a decrease above 9.4 T and that of Eu-**2** shows an increase in relaxivity from 3 to 7 T followed by a decrease above 7 T. This "bump" could be similar to the bump with a maximum value between 7 and 9.4 T observed at lower field strengths in the NMR dispersion plots of slowly rotating Gd^{3+}-based contrast agents.[16] An attempt to explain this increase in relaxivity at higher fields was made using a simulation of the Solomon–Bloembergen–Morgan (SBM) equations. Although the relaxivity values from this simulation matched the trend observed for GdDOTA, they did not fit the experimental data for Eu^{2+}-containing complexes. The results of this simulation indicate that SBM theory alone cannot explain our observations.

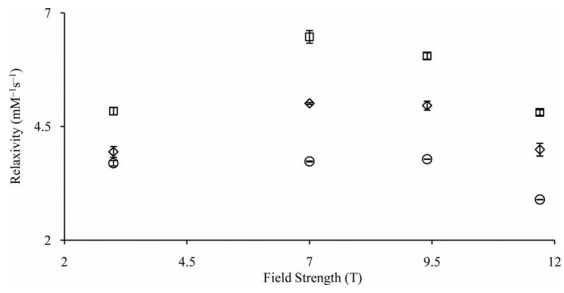

Figure 5. Proton longitudinal relaxivity (T = 20 °C, pH = 7.4) of GdDOTA (○), Eu-**1** (◇), and Eu-**2** (□) as a function of magnetic field strength. Values at 3, 7, and 11.7 T are from ref.[3] Error bars represent standard error of the mean.

At a higher temperature (T = 37 °C, pH = 7.4, Figure 6), Eu-**1** displays an increase in relaxivity from 1.4 to 7 T and a decrease above 9.4 T. However, at 37 °C, the relaxivity of Eu-**2** at 1.4 and 9.4 T is the same. At all field strengths and temperatures measured (except 1.4 T), Eu-**1** and Eu-**2** have higher relaxivities than GdDOTA. To further explain the influence of temperature on the relaxivity of Eu-**1** and Eu-**2**, we measured relaxivity as a function of temperature at a constant field strength.

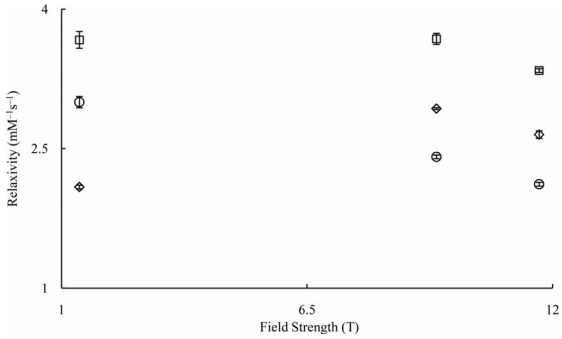

Figure 6. Proton longitudinal relaxivity (T = 37 °C, pH = 7.4) of GdDOTA (○), Eu-**1** (◇), and Eu-**2** (□) as a function of magnetic field strength. Values at 1.4 and 11.7 T are from ref.[3] Error bars represent standard error of the mean.

Influence of Temperature on Relaxivity

Temperature can have a dramatic influence on the relaxivity of contrast agents. To explore the temperature dependence of the relaxivity of Eu-**1** and Eu-**2**, we measured the relaxivity at 15, 20, 30, 37, and 50 °C at 9.4 and 11.7 T at pH = 7.4 (Figures 7 and 8).

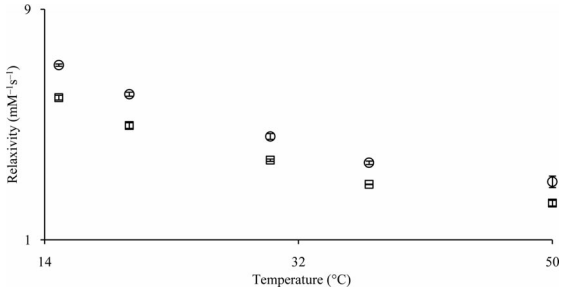

Figure 7. Proton longitudinal relaxivity (9.4 T and pH = 7.4) of Eu-**1** (□) and Eu-**2** (○) as a function of temperature. Error bars represent standard error of the mean.

The relaxivity of Eu-**1** and Eu-**2** decreased by 62 and 57%, respectively, at 9.4 T and 61 and 53%, respectively, at 11.7 T when the temperature increased from 15 to 50 °C. This drop in relaxivity is expected when the temperature is varied based on the Stokes–Einstein–Debye equation, which relates the rotational correlation rate to temperature.[17] For small molecules such as Eu-**1** and Eu-**2**, an important molecular parameter that affects relaxivity is the rotational correlation rate.[18] This parameter increases with temperature, thereby decreasing the relaxivity as predicted by SBM theory.[19]

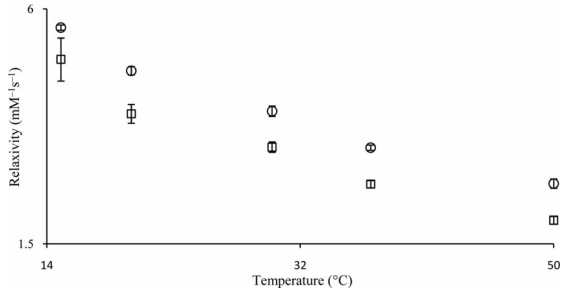

Figure 8. Proton longitudinal relaxivity (11.7 T, pH = 7.4) of Eu-**1** (□) and Eu-**2** (○) as a function of temperature. Error bars represent standard error of the mean.

Another temperature-dependent parameter that contributes to relaxivity is the water-exchange rate, which is important when it approaches the magnitude of the relaxation rate of the bound water. When this happens, the plot of relaxivity vs. temperature shows a plateau or a positive slope in the low temperature region. This was not observed for Eu-**1** or Eu-**2**, which implies that the water-exchange rates of Eu-**1** and Eu-**2** are fast enough to not limit relaxivity even at low temperatures. This conclusion is supported by the results of variable temperature ^{17}O NMR studies, which revealed that Eu-**1** and Eu-**2** have water-exchange rates of 3.3×10^8 and 0.85×10^8 s^{-1}, respectively.[3] In general, the variation in the relaxivities of these cryptates with temperature is likely due to the changes in the rotational correlation rate of the complexes as the temperature changes, similar to that observed for Gd^{3+}-containing complexes.

Influence of pH on Relaxivity

The effect of pH on the relaxivity of Eu^{2+}-containing cryptates was examined as a gauge of their performance in vivo and to explore the potential of these complexes to behave as pH responsive agents (Figure 9).

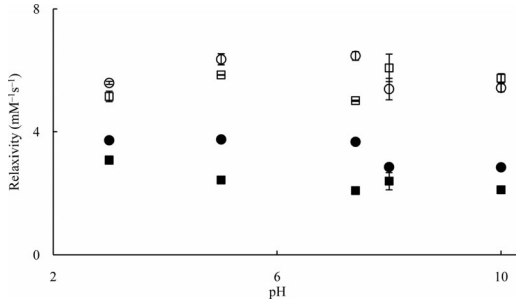

Figure 9. Longitudinal relaxivity at 1.4 T at 37 °C [Eu–**1** (■) and Eu–**2** (●)] and 7 T at 19 °C [Eu–**1** (□) and Eu–**2** (○)] as a function of pH. Error bars represent standard error of the mean.

At 7 T and 19 °C, the relaxivity of Eu-**1** did not change significantly at any of the pH values measured from 3–10 (α = 0.01), and that of Eu-**2** exhibited the same behavior. These observations are expected for complexes that do not have pH-sensitive functional groups. Also, at 1.4 T and

37 °C, the relaxivity of Eu-**1** is independent of the pH value (α = 0.01), whereas, the relaxivity of Eu-**2** remained constant below pH 7.4, but between pH 7.4 and 8, the relaxivity of Eu-**2** decreased by 22% (from 3.67 ± 0.09 to 2.86 ± 0.02 mM^{-1} s^{-1}) and remained constant above pH 8. In summary, the experiments at different pH values for Eu-**1** and Eu-**2** under two different sets of conditions (7 T at 19 °C and 1.4 T at 37 °C) indicate that the relaxivities of these cryptates are not influenced by pH over a physiologically relevant range.

Conclusions

Eu^{2+}-containing cryptates that have no amide moieties in their structures were kinetically stable in the presence of Ca^{2+}, Mg^{2+}, and Zn^{2+} at concentrations 1.87–20 times higher than biological concentrations. In addition, transmetallation studies demonstrated that the kinetic stability of Eu^{2+}-containing cryptates is affected by the presence of amides.

Relaxometric studies of Eu-**1** and Eu-**2** showed that the efficiencies of these cryptates were higher at 7 and 9.4 T at 20 °C. Furthermore, the relaxivities of these complexes decreased as the temperature increased from 15 to 50 °C, likely due to the increase in rotational correlation rate with increasing temperature. In addition, the efficacy of Eu-**1** and Eu-**2** did not vary significantly in the pH range of 3–10, which suggests that these complexes are expected to display constant relaxivity in biologically relevant pH ranges. These studies lay the foundation for the use of Eu^{2+}-containing cryptates as contrast agents for MRI, and we are currently pursuing synthetic modifications of these cryptates, thermodynamic stability and electron paramagnetic resonance spectroscopic measurements, and in vivo testing.

Experimental Section

General: Commercially available chemicals were of reagent-grade purity or better and were used without further purification unless otherwise noted. Water was purified using a PURELAB Ultra Mk2 water purification system (ELGA). Dicholoromethane was dried using a solvent purification system (Vacuum Atmospheres Company) and degassed under vacuum. Triethylamine was distilled from CaH_2 under an atmosphere of Ar.[20] Flash chromatography was performed using silica gel 60, 230–400 mesh (EMD Chemicals).[21] Analytical TLC was carried out with ASTM TLC plates precoated with silica gel 60 F_{254} (250 μm layer thickness). TLC visualization was accomplished using a UV lamp followed by charring with potassium permanganate stain (2 g of $KMnO_4$, 20 g of K_2CO_3, 5 mL of 5% w/v aqueous NaOH, 300 mL of H_2O). ^1H NMR spectra were obtained with a Varian Unity 400 (400 MHz) spectrometer, and ^{13}C NMR spectra were obtained with a Varian Unity 400 (101 MHz) spectrometer. Chemical shifts are reported relative to residual solvent signals ($CDCl_3$: ^1H: δ = 7.27, ^{13}C: δ = 77.23 ppm). ^1H NMR spectroscopic data are assumed to be first order, and the apparent multiplicity is reported as d = doublet and m = multiplet. HRMS (ESI) were obtained with an electrospray time-of-flight high-resolution Waters Micromass LCT Premier XE mass spectrometer. Samples for inductively coupled plasma mass spectrometry (ICP-MS) were diluted using aqueous nitric acid (2% v/v). Standard solutions were prepared by serial dilution of a Eu standard (High-Purity Standards). ICP-MS measurements were conducted with a PE Sciex Elan 9000 ICP-MS instrument with a cross-flow nebulizer and Scott-type spray chamber. Longitudinal relaxation times, T_1, were measured using standard receovery methods with a Bruker Minispec mq 60 [1.4 T] at 60 MHz and 37 °C, a Varian Unity 400 (9.4 T) at 400 MHz and 15, 20, 30, 37, and 50 °C, and a Varian 500S instrument (11.7 T) at 500 MHz and 15, 20, 30, 37, and 50 °C. A plot of $1/T_1$ vs. Eu concentration was performed to calculate relaxivity. In the measurements, four to five different concentrations including a blank were used, and measurements were repeated three times with independently prepared samples. Susceptibility weighted imaging (SWI) was performed at 3 (Siemens TRIO) and 7 T (ClinScan) using volume coils. The acquisition parameters were as follows: T_R = 37 ms, T_E = 5.68–31.18 ms, resolution: $0.5 \times 0.5 \times 2$ mm^3 for 3 T; T_R = 21 ms, T_E = 3.26–15.44 ms, resolution: $0.27 \times 0.27 \times 2$ mm^3 for 7 T. Multiple flip angles (5, 10, 15, 20, 25, and 30°) were used in the SWI experiments to allow the determination of T_1.[22] MR images were processed using SPIN software (SVN Revision 1751). Matlab (7.12.0.635 R2011a) was used to generate effective transverse relaxation time, T_2*, and corrected T_1 maps. The T_1 values from the corrected T_1 maps were plotted vs. the concentration of Eu in the samples to calculate longitudinal relaxivities, r_1, as previously reported.[3]

4,7,21,24-Tetraoxa-13,16-dithia-1,10-diazabicyclo[8.8.8]hexacosane-11,18-dione (3): A solution of (ethylenedithio)diacetic acid (0.500 g, 2.38 mmol) in thionyl chloride (5.0 mL, 68 mmol) under Ar was heated at reflux for 5 h. Excess thionyl chloride was removed under reduced pressure, and the residue was dissolved in anhydrous toluene (40 mL). The resulting solution and a solution of 1,4,10,13-tetraoxa-7,16-diazacyclooctadecane and triethylamine (1.5 mL, 0.010 mol, 4.2 equiv.) in anhydrous toluene (40 mL) were added simultaniously (50 mL/h) to a separate flask containing anhydrous toluene (100 mL) at 0–5 °C under an Ar atmosphere. The resulting solution was stirred for 12 h at ambient temperature. A yellow-orange suspension formed, which was filtered, and the solvent from the filtrate was removed under reduced pressure. Purification of the residue using silica gel chromatography (10:1 CH_2Cl_2/methanol) yielded **3** (0.215 g, 43%) as a fluffy yellow solid. ^1H NMR (400 MHz, $CDCl_3$): δ = 2.77–4.32 (m, CH_2) ppm. ^{13}C NMR (101 MHz, $CDCl_3$): δ = 32.9 (*C*H_2), 33.6 (*C*H_2), 49.7 (*C*H_2), 50.5 (*C*H_2), 69.2 (*C*H_2), 69.5 (*C*H_2), 71.2 (*C*H_2), 71.4 (*C*H_2), 170.7 ppm. TLC: R_f = 0.54 (10:1 CH_2Cl_2/methanol). HRMS (ESI): calcd. for $NaC_{18}H_{32}N_2S_2O_6$ $[M + Na]^+$ 459.1600; found 459.1602.

5,6-Benzo-4,7,13,16,20,23-hexaoxa-1,10-diazabicyclo[8.8.8]hexacosane-2,9-dione (4): A solution of catechole-1,4-*o,o*-diacetic acid (0.40 g, 1.8 mmol) in thionyl chloride (5.0 mL, 68 mmol) under Ar was heated at reflux for 5 h. Excess thionyl chloride was removed under reduced pressure, and the residue was dissolved in anhydrous toluene (25 mL). The resulting solution and a solution of 1,4,10,13-tetraoxa-7,16-diazacyclooctadecane (0.32 g, 1.2 mmol, 1.0 equiv.) and triethylamine (0.50 mL, 3.3 mmol, 2.4 equiv.) in anhydrous toluene (25 mL) were added simultaniously (50 mL/h) to a separate flask containing anhydrous toluene (60 mL) at 0–5 °C under an Ar atmosphere. The solution was stirred for 12 h at ambient temperature. An orange suspension formed, which was filtered, and the solvent was removed under reduced pressure. Purification of the residue using silica gel chromatography (9:1 CH_2Cl_2/methanol) yielded **4** (0.144 g, 36%) as a fluffy white solid. ^1H NMR (400 MHz, $CDCl_3$): δ = 2.77–3.22 (m, 2 H, CH_2), 3.37–3.83 (m, 20 H, CH_2), 4.08–4.35 (m, 2 H, CH_2), 4.64–4.91 (m, 2 H, CH_2), 5.15–5.23 (d, J = 14.4 Hz, 2 H, CH_2), 6.86–7.10 (m, 4 H, C*H*) ppm. ^{13}C NMR (101 MHz, $CDCl_3$): δ = 48.5 (*C*H_2),

48.9 (CH_2), 68.1 (CH_2), 69.4 (CH_2), 69.7 (CH_2), 71.1 (CH_2), 71.3 (CH_2), 116.1 (CH), 122.2 (CH), 148.3, 169.0 ppm. TLC: R_f = 0.8 (9:1 CH_2Cl_2/methanol). HRMS (ESI): calcd. for $NaC_{22}H_{32}N_2O_8$ [M + Na]$^+$ 475.2062; found 475.2060.

General Procedure for the Synthesis of Eu-1–4: A degassed aqueous solution of $EuCl_2$ (1 equiv.) was mixed with a degassed aqueous solution of a cryptand (2 equiv.). The resulting mixture was stirred for 12 h at ambient temperature under Ar. Degassed PBS (10×) was added, and stirring was continued for 30 min. The concentration of Eu in the resulting solution was verified by ICP-MS, and the solution was used directly for relaxivity measurements. For transmetallation experiments, the same procedure was followed with only 1 equiv. of ligand.

pH Buffers: The following commercially available buffers were degassed and used in relaxometric experiments: glycine/HCl (pH = 3), acetate (pH = 5), PBS (pH = 7.4), 2-amino-2-(hydroxymethyl)propane-1,3-diol (TRIS) (pH = 8), and glycine/NaOH (pH = 10).

Transmetallation Kinetics: The following procedure was adapted from Muller and coworkers.[9] A stock solution of the Eu^{2+}-containing cryptate (5 mM) was prepared in degassed PBS. To an aliquot of this solution was added a solution of Ca^{2+} (12.1 mM) in degassed PBS such that the resulting solution was 2.5 mM in both Eu^{2+} and Ca^{2+}. This solution was stirred at 37 °C under Ar. Aliquots were taken at 90, 180, 420, 1500, 3300, and 4740 min after the addition of Ca^{2+}. All aliquots were filtered using 0.2 μm filters prior to T_1 measurements. The t_1 value of these aliquots (60 MHz, 37 °C) was immediately measured at each time point. The experiment was triplicated with independently prepared solutions. The entire procedure was repeated using Mg^{2+} (16.4 mM) and Zn^{2+} (9.97 mM) in place of Ca^{2+} (12.1 mM). Stastical analysis of variance was performed using the program found at faculty.vassar.edu/lowry/anova1u.html.

Supporting Information (see footnote on the first page of this article): ^1H and ^{13}C NMR spectra of **3** and **4**.

Acknowledgments

This research was supported by startup funds from Wayne State University (WSU) and by the National Institute of Biomedical Imaging and Bioengineering of the National Institutes of Health (Pathway to Independence Career Transition Award, R00EB007129). J. G. was supported by a Paul and Carol Schaap Graduate Fellowship, and M. J. A. gratefully acknowledges a Schaap Faculty Scholar Award. We thank Latif Zahid and Yimin Shen for performing imaging experiments.

[1] P. Caravan, C. T. Farrar, L. Frullano, R. Uppal, *Contrast Media Mol. Imaging* **2009**, *4*, 89–100.
[2] a) L. Burai, R. Scopelliti, É. Tóth, *Chem. Commun.* **2002**, 2366–2367; b) É. Tóth, L. Burai, A. E. Merbach, *Coord. Chem. Rev.* **2001**, *216–217*, 363–382; c) P. Caravan, É. Tóth, A. Rockenbauer, A. E. Merbach, *J. Am. Chem. Soc.* **1999**, *121*, 10403–10409.
[3] J. Garcia, J. Neelavalli, E. M. Haacke, M. J. Allen, *Chem. Commun.* **2011**, *47*, 12858–12860.
[4] E. L. Yee, O. A. Gansow, M. J. Weaver, *J. Am. Chem. Soc.* **1980**, *102*, 2278–2285.
[5] a) J. M. Wolfson, D. R. Kearns, *Biochemistry* **1975**, *14*, 1436–1444; b) Y. Ogawa, S. Suzuki, K. Naito, M. Saito, E. Kamata, A. Hirose, A. Ono, T. Kaneko, M. Chiba, Y. Inaba, Y. Kurokawa, *J. Environ. Pathol. Toxicol. Oncol.* **1995**, *14*, 1–9.
[6] J. H. Burns, C. F. Baes Jr., *Inorg. Chem.* **1981**, *20*, 616–619.
[7] a) J. G. Penfield, R. F. Reilly Jr., *Nat. Clin. Pract. Nephrol.* **2007**, *3*, 654–668; b) M. F. Tweedle, P. Wedeking, K. Kumar, *Invest. Radiol.* **1995**, *30*, 372–380.
[8] N.-D. H. Gamage, Y. Mei, J. Garcia, M. J. Allen, *Angew. Chem. Int. Ed.* **2010**, *49*, 8923–8925.
[9] S. Laurent, L. Vander Elst, C. Henoumont, R. N. Muller, *Contrast Media Mol. Imaging* **2010**, *5*, 305–308.
[10] a) B. Deng, P. Zhu, Y. Wang, J. Feng, X. Li, X. Xu, H. Lu, Q. Xu, *Anal. Chem.* **2008**, *80*, 5721–5726; b) S. Pors Nielsen, *Scand. J. Clin. Lab. Invest.* **1969**, *23*, 219–225.
[11] S. Laurent, L. Vander Elst, R. N. Muller, *Contrast Media Mol. Imaging* **2006**, *1*, 128–137.
[12] A xylenol orange-based colorimetric assay was used to test for the presence of free europium as described in ref.[14] When a solution of $EuCl_2$ (2.5 mM) in PBS was prepared, a precipitate immediately formed. The filtrate of the mixture was exposed to air to allow oxidation of Eu^{2+} to Eu^{3+}, and the Eu^{3+} concentration was measured with xylenol orange as an indicator using a calibration curve made from a purchased Eu standard. A concentration of 1.63 μM was measured, which corresponds to 0.07% of the original Eu in solution.
[13] a) J. Kowalewski, A. Egorov, D. Kruk, A. Laaksonen, S. Nikkhou Aski, G. Parigi, P.-O. Westlund, *J. Magn. Reson.* **2008**, *195*, 103–111; b) D. Kruk, J. Kowalewski, *J. Chem. Phys.* **2002**, *116*, 4079–4086; c) T. Nilsson, G. Parigi, J. Kowalewski, *J. Phys. Chem. A* **2002**, *106*, 4476–4488; d) J. Svoboda, T. Nilsson, J. Kowalewski, P.-O. Westlund, P. T. Larsson, *J. Magn. Reson., Ser. A* **1996**, *121*, 108–113.
[14] D. J. Averill, J. Garcia, B. N. Siriwardena-Mahanama, S. M. Vithanarachchi, M. J. Allen, *J. Vis. Exp.* **2011**, *53*, e2844.
[15] a) K. W.-Y. Chan, W.-T. Wong, *Coord. Chem. Rev.* **2007**, *251*, 2428–2451; b) D. E. Reichert, R. D. Hancock, M. J. Welch, *Inorg. Chem.* **1996**, *35*, 7013–7020.
[16] L. Helm, *Future Med. Chem.* **2010**, *2*, 385–396.
[17] R. M. Anderton, J. F. Kauffman, *J. Phys. Chem.* **1994**, *98*, 12117–12124.
[18] P. Caravan, *Chem. Soc. Rev.* **2006**, *35*, 512–523.
[19] P. Caravan, J. J. Ellison, T. J. McMurry, R. B. Lauffer, *Chem. Rev.* **1999**, *99*, 2293–2352.
[20] W. L. F. Armarego, C. L. L. Chai, in: *Purification of Laboratory Chemicals, Fifth Edition*, Elsevier, Burlington, MA, **2003** p. 375.
[21] W. C. Still, M. Kahn, A. Mitra, *J. Org. Chem.* **1978**, *43*, 2923–2925.
[22] E. M. Haacke, R. W. Brown, M. R. Thompson, R. Venkatesan, in: *Magnetic Resonance Imaging Physical Principles and Sequence Design*, John Wiley & Sons, Inc., New York, **1999**, p. 654.

Received: October 21, 2011
Published Online: February 8, 2012

